Bull Math Biol (2017) 79:2627–2648
DOI 10.1007/s11538-017-0344-8

Society for Mathematical Biology

ORIGINAL ARTICLE

Continuous Structured Population Models for *Daphnia magna*

Erica M. Rutter[1] · **H. T. Banks**[1] · **Gerald A. LeBlanc**[2] · **Kevin B. Flores**[1]

Received: 21 December 2016 / Accepted: 5 September 2017 / Published online: 15 September 2017

Abstract We continue our efforts in modeling *Daphnia magna*, a species of water flea, by proposing a continuously structured population model incorporating density-dependent and density-independent fecundity and mortality rates. We collected new individual-level data to parameterize the individual demographics relating food availability and individual daphnid growth. Our model is fit to experimental data using the generalized least-squares framework, and we use cross-validation and Akaike Information Criteria to select hyper-parameters. We present our confidence intervals on parameter estimates.

Keywords Continuous structured population models · Inverse problems · Generalized least squares · Model selection · Information content · Residual plots

1 Introduction

Structured population models (SPMs) track the density of a population of individuals over time with respect to a physiologically structured variable, such as age or size. SPMs have been used to describe a wide variety of ecological data, see Caswell (1989, 2005), Diekmann et al. (2007), Keyfitz and Caswell (2005), Ellner et al. (2016), Ellner

Electronic supplementary material The online version of this article (doi:10.1007/s11538-017-0344-8) contains supplementary material, which is available to authorized users.

✉ Erica M. Rutter
erutter@ncsu.edu

1 Department of Mathematics, Center for Research in Scientific Computation, North Carolina State University, Raleigh, NC 27695, USA

2 Department of Biological Sciences, North Carolina State University, Raleigh, NC 27695, USA

and Guckenheimer (2011) and the references therein. SPMs are desirable because they describe the life history of the organism and allow for dependence of age or density on growth, survival, and fecundity rates. SPMs can be both discretely structured (Leslie 1945) or continuously structured (Sinko and Streifer 1967).

A continuously structured population model can be preferable to a discrete model for several reasons. When using discrete structured population models (SPMs), parameter estimation may be computationally unstable when parameters are time or age-dependent (Banks et al. 2009; Wood 1994). Previous work (Banks et al. 2007, 2008) has indicated that the Sinko–Streifer model (Sinko and Streifer 1967), a continuously structured population model, is more amenable to estimating age-dependent parameters than discretely structured models. Further, we have previously (Adoteye et al. 2015a) compared discrete and continuous SPMs for the density-independent *Daphnia magna* survival data and found that the Sinko–Streifer model generated a better fit to data.

Daphnia magna is a species of water flea that has been widely studied in ecotoxicology due to their ability to quickly reproduce and their sensitivity to exogenous chemicals. Daphnids are often used to gauge the hazard of pesticides or other chemicals on the ecosystem (LeBlanc et al. 2013; Rider and LeBlanc 2005; Wang et al. 2005, 2011). Ecological risk assessments that use daphnids are most commonly performed at the organismal response. However, organismal response level does not directly correlate to population-level responses nor does it allow for causal association to ecosystem adversity, which remains of interest to toxicologists (Council 2013). Mathematical models may be used to quantitatively connect organismal assessment information to the population level (Ankley et al. 2010; Council 2013; Hanson and Stark 2011). Recent daphnid structured population modeling efforts have lacked age-dependent demographics (Erickson et al. 2014), an estimation of density-dependent parameter uncertainty, or have focused on qualitative model analysis instead of model validation (Diekmann et al. 2010; El-Doma 2011, 2012; Farkas and Hagen 2007; Kramer et al. 2011). Thus, current daphnia SPMs do not accurately capture the long-term dynamics of aggregate (Banks et al. 2014) population data.

It has long been suggested that daphnid growth is dependent upon food availability (Kooijman and Metz 1984). In particular, duration of the juvenile stage may be dependent on quantity of available resources (Nisbet and Gurney 1983). Previous mathematical models (de Roos et al. 1990) argue that dependence of growth on food availability allows for limit cycle emergence and oscillatory behavior. Corresponding mathematical models have incorporated resource-dependent growth, fecundity and mortality (Ananthasubramaniam et al. 2011). Nelson et al. (2007) introduced a stage-structured model incorporating juveniles, adults, and algae. Using this model, McCauley et al. (2008) discovered that the coexistence of large-amplitude fluctuations with small amplitude cycles in consumer-resource systems may be due to delayed juvenile stage duration. However, although these previous models are well formulated and mathematical analysis was performed, they did not include fitting the models to longitudinal experimental data. In addition, these models do not consider the other effects of density dependence, such as the accumulation of metabolites in the media resulting from overcrowding, which has been shown to

influence daphnid fecundity (Goser and Ratte 1994). Preuss et al. (2009) investigated these density-dependent effects in an individual-based model and discovered that, in addition to intraspecific competition, crowding effects must be incorporated.

We propose a continuously structured SPM for *Daphnia magna* that includes both density-independent and density-dependent growth, fecundity, and mortality. We perform individual-level experiments determining the effect of food restriction on daphnid growth to inform our model. We fit our model to *Daphnia magna* data using a vector generalized least-squares framework and perform cross-validation. We determine local sensitivities on all estimated parameters to understand how the model is affected by parameter changes. Further, we calculate confidence intervals and standard errors for our parameters. We also propose a slight variation on our model, allowing for more flexibility in the relationship between density-dependent mortality and biomass. We estimate the additional parameters and show, using the Akaike Information Criteria score, that the more complex model does not perform better than the simpler model. We also obtain realistic confidence intervals using the simpler model.

2 Mathematical Model

We employ the Sinko–Streifer equations (1967) that describe the continuous-time dynamics of a population structured over a continuous variable, which in this case we take to be age (a). $u(t, a)$ represents the population at time t of age a.

$$\frac{\partial u(t,a)}{\partial t} + \frac{\partial u(t,a)}{\partial a} = -\mu_{\text{ind}}(a)\mu_{\text{dep}}(a, M(t))u(t,a) \tag{1}$$

The mortality rate is a product of a density-independent rate, $\mu_{\text{ind}}(a)$, and a density-dependent rate $\mu_{\text{dep}}(a, M(t))$. The density-dependent rate depends on age as well as total biomass at time t, given by $M(t)$. The density-dependent rate is a dimensionless scaling factor that changes with the biomass. This function is intended to describe the effects of food availability as well as other factors that may influence the survival, such as overcrowding (Goser and Ratte 1994). Our boundary condition represents the introduction of neonates into the population and is given by:

$$u(t,0) = \int_0^{a_{\max}} k_{\text{ind}}(s)k_{\text{dep}}(M(t-\tau))u(t,s)\mathrm{d}s \tag{2}$$

The fecundity kernel in the recruitment term is similarly described by density-independent and density-dependent rates. The density-dependent rate is dimensionless and scales the density-independent rate with the increase in biomass. This rate describes the effects of crowding, such as lower algae levels or other resource scarcities. Following the assumptions validated in previous results (Adoteye et al. 2015b), the density-dependent rate is delayed and depends on the biomass τ days ago.

The equation describing total population biomass is given by:

$$M(t) = \int_0^{a_{\max}} u(t,s) \left(\frac{K M_0 e^{rs}}{K + M_0(e^{rs} - 1)} \right)^L \mathrm{d}s. \tag{3}$$

where L represents the exponent that relates daphnid length to daphnid biomass. Based on previous results (Adoteye et al. 2015b), and results explained in Sect. 3.1, the length of each daphnid is assumed to follow a logistic growth curve. We model biomass as daphnid length raised to an exponent L, since daphnia mass typically varies allometrically with length with the exponent having a value between 2 and 3 (de Roos et al. 1990). We then integrate over all ages in order to obtain the total biomass of the population.

We assume that the density-dependent rate of mortality is a non-decreasing function of population biomass, i.e., $\frac{\partial \mu_{\text{dep}}}{\partial M} \geq 0$, and that it is a non-increasing function of age, i.e., $\frac{\partial \mu_{\text{dep}}}{\partial a} < 0$. We use a hill function to describe the effect of age and a linear function to describe the effect of biomass:

$$\mu_{\text{dep}}(a, M(t)) = 1 + c_1 M(t) \frac{c_3^{h_2}}{c_3^{h_2} + a^{h_2}}. \tag{4}$$

We make the additional assumption that μ_{dep} only affects non-reproductive individuals and has no effect on reproductive individuals (adults). To model this assumption, we take $c_3 = 8$ days old (the age just before the first offspring are produced) and the hill coefficient $h_2 = 10$, which describes a sharp cutoff in the age at which density has an effect on mortality.

We assume that the density-dependent rate of fecundity is a non-increasing function of population biomass, i.e., $\frac{\partial k_{\text{dep}}}{\partial M} \leq 0$. To model this behavior, we used the following hill function:

$$k_{\text{dep}}(M(t-\tau)) = \frac{q^{h_3}}{q^{h_3} + M(t-\tau)^{h_3}} \tag{5}$$

This functional form is chosen in order to describe a monotone decreasing dependence of fecundity on biomass that is biologically relevant, i.e., the total fecundity rate $k = k_{\text{ind}} k_{\text{dep}}$ equals k_{ind} when $M(t) = 0$ and is approximately zero for sufficiently large $M(t)$.

The density-independent rates of fecundity and mortality were estimated from individual-level data (Adoteye et al. 2015b), further explained in Sect. 3.1. The daily data for density-independent fecundity were used to directly parameterize the density-independent fecundity, $k_{\text{ind}}(a)$, as a function of age. For $\mu_{\text{ind}}(a)$, we used an age-varying function that we previously estimated (Adoteye et al. 2015a) within a density-independent Sinko–Streifer framework using piecewise linear splines (Banks and Davis 2007).

The observables for the data set we collected are the total counts of daphnids within two size classes, which are described by an age cutoff a_1 that we previously determined

by estimating the relationship between age and size (Adoteye et al. 2015b):

$$S_1(t) = \int_0^{a_1} u(t, s)\mathrm{d}s \tag{6}$$

$$S_2(t) = \int_{a_1}^{a_{\max}} u(t, s)\mathrm{d}s \tag{7}$$

The total population size is the sum of $S_1(t)$ and $S_2(t)$, or

$$N(t) = \int_0^{a_{\max}} u(t, s)\mathrm{d}s \tag{8}$$

The integral in these population counts ends at a specified age, $a_{\max}$, which we take to be 90 days. This limit is older than the last surviving daphnid we found in density-independent experiments, and allows for finitely defined age-mesh in the numerical PDE solver.

3 Methods

3.1 Data

The population data used to fit our model are obtained as previously described in Adoteye et al. (2015b), but here we will briefly describe the data for completeness. A longitudinal study was performed, in duplicate, over 102 days. The daphnid media, reconstituted from deionized water as previously described (Baldwin and LeBlanc 1994), was seeded with five 6-day-old female daphnids. Daphnids were counted every Monday, Wednesday and Friday for the first three weeks of the experiment and weekly thereafter. Daphnia were separated into two size classes with a fine-mesh 1.62-mm-pore-size net.

The parameters used for density-independent rates are based on individual-level experiments also described in Adoteye et al. (2015b). Thirty individual daphnids were housed in 50-mL beakers containing 40 mL of daphnid media. They had media changed daily and were being fed 7×10^6 cells of algae (*Pseudokirchneriella subcapita*) and 0.5 mg (dry weight) of Tetrafin™ fish food. This amount of food differs from laboratory conditions and was inspired by previous work (Olmstead and LeBlanc 2007). Major axis length as well as fecundity were measured daily until all daphnids had died (after 74 days). The major axis lengths were fit to a logistic curve individually to determine parameters r, K, and M_0 (Adoteye et al. 2015b).

We subsequently performed a 14-day individual experiment to assess the effects that food restriction had on daphnid growth and, consequently, biomass, defined in Eq. (3). Although previous experimental work has shown that the major axis length of adult daphnids decreases with food restriction, exact experimental procedures or data were not included (Kooijman and Metz 1984). We tested 3 food levels: our laboratory control (receiving 1.12×10^7 cells of algae (*Pseudokirchneriella subcapita*) and 0.8 mg Tetrafin™ fish food daily), a medium food group (receiving 3.5×10^6 cells

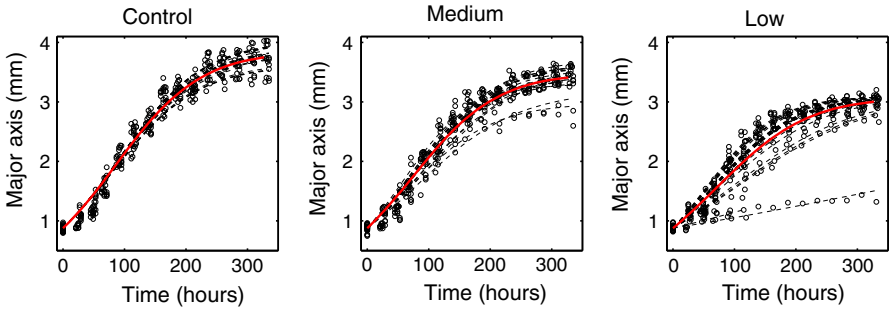

Fig. 1 (Color figure online) Results from the individual-level study of food restriction on daphnid growth. Black circles represent data points from each individual daphnid. The red line represents the mean fit to a logistic curve. The black dashed lines represent the logistic curve fit to each individual daphnid

of algae daily with 0.25 mg Tetrafin™ fish food), and a low food group (receiving 1.75×10^6 cells of algae daily with 0.125 mg Tetrafin™ fish food). All preceding fish food measurements are by dry weight. Fish food was prepared by blending 4mg of Tetrafin™ fish food with 400 mL of water. Feedings were split in half, occurring at 10 am and 5 pm daily. Media changes occurred daily at 9 am. Each of these food level experiments contained 28 individual daphnids, housed in 40 mL of daphnid media in 50 mL beakers. Neonates were harvested within 2 hours of being born. Daphnid major and minor axis lengths were measured daily at 9 am. We used a microscope camera (Handheld Digital Microscope Pro, 44308, Celestron, Torrance, California, USA) to take individual photos of each daphnid and the associated software to measure major and minor axis lengths. Online resource 1 contains a spreadsheet of all measurements. All associated pictures and measurements are available on the Open Science Framework (https://osf.io/vnm2x/).

Figure 1 depicts the lengths of individual daphnids as a function of time. We tested for differences in growth rate and adult size between the control food group, the medium food group, and the low food group. We fit the individual data to logistic curves, since previous results indicated that the logistic curve fit individual daphnid length better than other models, including the Gompertz equation, a constant, and linear equations (Adoteye et al. 2015b).

We used a nonlinear mixed effects modeling framework as described in Davidian and Giltinan (1995). This hierarchical nonlinear model consists of two stages: estimating the intra-individual parameters and variances followed by estimating the inter-individual parameters and variances. The goal is to determine the mean values of our parameters (r and K) over the population of daphnids, as well as their variance. The intra-individual statistical model is given by:

$$y_i = f_i(\beta_i) + e_i \tag{9}$$

where i represents the individual, y_i is the response of the ith individual, f_i is the logistic function, β_i are the parameters being estimated for individual i (in this case $\beta_i = (r_i, K_i)$). e_i is the random intra-individual errors for the ith individual and is assumed that $(e_i|\beta_i) \sim \mathcal{N}(0, C)$, where C represents the covariances. Secondly,

Table 1 Mean parameter estimates and variances along with individual daphnid parameter estimates for the logistic equation using a nonlinear mixed effects model for the Adoteye et al. (2015b) food group, the control food group, the medium food group, and the low food group

Food group	Parameter	K	r	M_0
Adoteye et al. (2015b)	Fixed effect mean value	3.7346	0.0157	0.7333
	Random effect variance	0.0010533	0.0048239	6.8978×10^{-7}
Control	Fixed effect mean value	3.8675	0.014398	0.8771
	Random effect variance	0.024703	2.4357×10^{-9}	–
Medium food	Fixed effect mean value	3.4899	0.014718	0.8771
	Random effect variance	0.036451	2.1267×10^{-6}	–
Low food	Fixed effect mean value	3.1032	0.013315	0.8771
	Random effect variance	6.6215×10^{-8}	1.5134×10^{-5}	–

we assume that inter-individual variation is due to random effects, resulting in the following model for β_i:

$$\beta_i = \beta + b_i \tag{10}$$

where β is the fixed effects (mean of all the β_i), and b_i, the random effects that vary in the population. It is assumed $b_i \sim \mathcal{N}(0, D)$ where D is a covariance matrix. Here, we assume the covariance between r and K is zero and, thus, D is a diagonal matrix. The diagonal entries of D form our random effect variances in Table 1. We used MATLAB's NLMEFIT function to perform our estimates of β and b_i.

In contrast to the values found in Adoteye et al. (2015b), the initial condition M_0 was assumed to be equal to the mean of the initial lengths of all daphnids, since this resulted in the lowest residual mean squared error for each group. Using a one-way T-test, we found that, although the K values were significantly different for each food group ($p < 0.01$), the growth rate, r, was not. Estimates of the population mean values of r, K, and M_0 and their associated random effect variances for each food group are given in Table 1.

3.2 Generalized Least-Squares Parameter Estimation and Uncertainties

In order to fit the model to our available data, we use a vector generalized least-squares (GLS) approach outlined in Banks et al. (2014) and Banks and Tran (2009). We calculate the total number of daphnids in each size class: size class one is $S_1(t,\theta) = \int_0^{a_1} u(t,s)\mathrm{d}s$, and size class two is $S_2(t,\theta) = \int_{a_1}^{a_{\max}} u(t,s)\mathrm{d}s$. Our forward solution observations for a set of parameters $\boldsymbol{\theta}$ is given by the vector $\boldsymbol{f}(t,\boldsymbol{\theta}) = [S_1(t,\boldsymbol{\theta}), S_2(t,\boldsymbol{\theta})]^T$.

The statistical model we consider allows proportional errors and has the form (here N is the number of observations)

$$\boldsymbol{Y}_j = \boldsymbol{f}(t_j;\boldsymbol{\theta}) + \boldsymbol{f}^{\gamma}(t_j;\boldsymbol{\theta})\mathcal{E}_j, \quad j = 1, 2, \ldots, N, \tag{11}$$

where $\mathcal{E}_j$ are independent and identically distributed (*i.i.d.*) with zero mean and covariance $V_0 = \text{diag}(\sigma_{01}^2, \sigma_{02}^2)$. We estimate our parameters by seeking to minimize a weighted least squares

$$\sum_{j=1}^{N} \boldsymbol{w}_j \left[\boldsymbol{y}_j - \boldsymbol{f}(t_j;\boldsymbol{\theta})\right]^2 \tag{12}$$

where $\boldsymbol{y}_j$ are the data and the weights $\boldsymbol{w}_j$ depend on $\boldsymbol{\theta}$. This leads to the so-called generalized least squares (GLS) formulation defined by the solution to the *normal equations*

$$\sum_{j=1}^{N} \left[\boldsymbol{y}_j - \boldsymbol{f}(t_j;\boldsymbol{\theta})\right]^T V^{-1}(t_j;\boldsymbol{\theta}) \nabla_{\theta_k} \boldsymbol{f}(t_j;\boldsymbol{\theta}) = 0, \quad k = 1, \ldots, \kappa_\theta, \tag{13}$$

where κ_θ is the number of parameters being estimated. We define

$$V(t_j;\boldsymbol{\theta}) = \text{diag}\left(f_1(t_j;\boldsymbol{\theta})^{2\gamma_1}\hat{\sigma}_{01}^2,\, f_2(t_j;\boldsymbol{\theta})^{2\gamma_2}\hat{\sigma}_{02}^2\right) \tag{14}$$

and

$$\hat{\sigma}_{0i}^2 = \frac{1}{N-\kappa_\theta} \sum_{j=1}^{N} \left(\frac{y_j^i - f_i(t_j;\boldsymbol{\theta})}{f_i(t_j;\boldsymbol{\theta})^{\gamma_i}}\right)^2, \quad i = 1, 2, \tag{15}$$

see Sections 3.2.5 and 3.2.6 of Banks et al. (2014). The iterative algorithm we use is further explained in Banks et al. (2014) and Banks and Tran (2009). We note that in the case of $\gamma = 0$, this reduces to the vectorized ordinary least squares.

Using asymptotic theory (Banks and Tran 2009; Banks et al. 2014), the vector generalized least-squares (GLS) estimator has a limiting distribution: $\boldsymbol{\theta}_{\text{GLS}} \sim \mathcal{N}(\boldsymbol{\theta}_0, \Sigma_0^N)$ using the true parameter values $\boldsymbol{\theta}_0$. Since these are unknown, we can approximate using our estimated parameter vector, $\hat{\boldsymbol{\theta}}$, and obtain $\boldsymbol{\theta}_{\text{GLS}} \sim \mathcal{N}(\boldsymbol{\theta}_0, \Sigma_0^N) \approx \mathcal{N}(\hat{\boldsymbol{\theta}}, \hat{\Sigma}^N)$ where

$$\hat{\Sigma}^N \approx \left(\sum_{j=1}^{N} D_j^T(\hat{\boldsymbol{\theta}}) V(t_j;\hat{\boldsymbol{\theta}}) D_j(\hat{\boldsymbol{\theta}})\right)^{-1} \tag{16}$$

with

$$D_j = \begin{pmatrix} \frac{\partial f_1(t_j;\hat{\boldsymbol{\theta}})}{\partial \theta_1} & \cdots & \frac{\partial f_1(t_j;\hat{\boldsymbol{\theta}})}{\partial \theta_{\kappa_\theta}} \\ \frac{\partial f_2(t_j;\hat{\boldsymbol{\theta}})}{\partial \theta_1} & \cdots & \frac{\partial f_2(t_j;\hat{\boldsymbol{\theta}})}{\partial \theta_{\kappa_\theta}} \end{pmatrix}.$$

and $V(t_j;\boldsymbol{\theta})$ as defined above. We use our optimized estimates $\hat{\boldsymbol{\theta}}$ from Eq. (13). From this distribution, we can obtain standard errors and 95% confidence intervals

Table 2 Fixed parameter values for the model

Parameter	Value
a_1	3 days
c_3	8 days
h_2	10
h_3	2

to quantify the uncertainty in the estimation of each parameter. Standard errors for each parameter i are given by $\mathrm{SE}(\hat{\theta}_i) = \sqrt{\hat{\Sigma}^N_{ii}}$. These standard errors (Banks and Tran 2009) are then used to create a 95% confidence interval around each parameter as $[\hat{\theta}_i - 1.96\mathrm{SE}(\hat{\theta}_i), \hat{\theta}_i + 1.96\mathrm{SE}(\hat{\theta}_i)]$.

In order to determine the correct statistical error model, in terms of which value of γ to use, we look towards finite differencing of the data as previously described in Banks et al. (2015). The advantage of this method is that we are able to examine pseudo-error residuals with respect to time and do not introduce bias associated with model error. We examine the second-order differencing of the data (the so-called pseudo-errors discussed in Banks et al. (2015)

$$\hat{\epsilon}_i = \frac{1}{\sqrt{6}}\left(y_{i+1} - 2y_i + y_{i-1}\right) \tag{17}$$

From this estimation of measurement errors, we then can define our modified pseudo-errors by:

$$\eta = \frac{\hat{\epsilon}_i}{|y_i - \hat{\epsilon}_i|^\gamma}. \tag{18}$$

Here, $\gamma = 0$ corresponds to vector ordinary least squares and $\gamma \neq 0$ represents generalized least squares. We separate our replicate data into size classes 1 and 2 and calculated the modified residuals using Eq. (18) for various values of γ.

Figure 2 depicts the modified residuals for each replicate for both the size class 1 and 2 populations. The best statistical model is chosen for plots where the distribution of points appears random. We note that for size class 1, the juveniles, a value of $\gamma = 0.5$ appears to be the most random. We reject $\gamma = 0$ for size class 1 because the magnitude of the residuals appear to be correlated with time. For size class 2, the adult population, however, $\gamma = 0$ is sufficiently random. We note that other works have incorporated varying γ values for certain classes of observables (Baraldi et al. 2014; Banks et al. 2016).

We only optimize over a subset of our parameter space. The fixed parameters for the model are given in Table 2. The parameters in the hill function describing the density-dependent death rate (Eq. 4) for size class 1 include the age at which the density dependent falls to 0 for 8-day-old daphnids (c_3) very steeply (h_2). For the parameters in the density-dependent fecundity rate (Eq. 5), only h_3, the power of the hill function, is fixed.

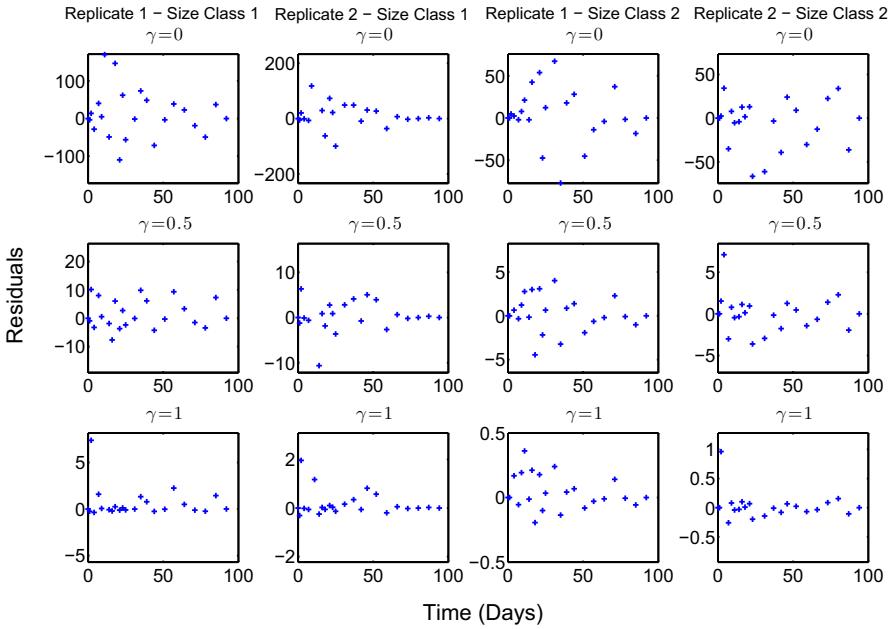

Fig. 2 (Color figure online) Modified residuals calculated by Eq. (18). Each column represents either size class 1 (left) or size class two (right). Each row represents results for a constant value of γ, including $\gamma = 0$ (top row), $\gamma = 0.5$ (middle row), and $\gamma = 1$ (bottom row)

Parameters K, r, and M_0 describe how individual daphnids contribute to the population biomass, i.e., total length $M(t)$, as described in Eq. (3). The information for these parameters is given in Table 1. The various parts of the table describe the values on the control, medium, and low food settings described in Sect. 3.1, as well as the r, K, and M_0 values previously measured in Adoteye et al. (2015b). Due to the small variances, all daphnids within a simulation will use the same r, K, and M_0 parameters from Table 1.

The parameters that are optimized via the above vector generalized least-squares framework are τ, the time delay for the effect of density on fecundity, L, the exponent relating daphnid length to biomass, q, the half-maximum for the effect of density on fecundity, and c_1, the slope of the linear relationship between density-dependent mortality and total mass, $M(t)$. Additionally, we repeated the optimizations for all various food levels.

The model equations are solved numerically in MATLAB using the hpde package (Shampine 2005). In order to perform the optimization, we will need an initial guess for MATLAB's LSQNONLIN. We use direct search (Finkel and Kelley 2004), a non-gradient-based algorithm, in order to obtain a suitable initial guess. Direct search requires upper and lower limits for the parameters, which we choose to be 10^{-10} and 1000, respectively. The optimization is performed until parameter values change by less than 0.1%.

3.3 Cross-Validation

Previous work indicated that $\tau > 6$ provided the best fit to population data (Adoteye et al. 2015b). Here, we perform a cross-validation over our two replicates to determine the best value of our hyper-parameters, τ and L to use in our optimization. We allow τ to vary in integer values from 6 to 24 and L to vary in integer values from 1 to 3. Integer values were chosen because of the prohibitive computational costs associated with a finer grid.

If we look over our entire data domain $D = \{d_1, d_2\}$, where each d_i is our replicate data, our best fit for a given value of τ is generated by the parameters $\hat{\theta} = (\hat{q}, \hat{c_1})$ that minimize the residual sum of squares (RSS) and has a value R_{fit}:

$$R_{\text{fit}}(\tau, L) = \min_{\theta}[\text{RSS}(D, \theta, \tau, L)] \tag{19}$$

$$\hat{\theta}(\tau, L) = \underset{\theta}{\text{argmin}}[\text{RSS}(D, \theta, \tau, L)] \tag{20}$$

Since we have two replicates of data, we can independently determine the parameter optimizations on each data set:

$$\hat{\theta}_i(\tau, L) = \underset{\theta}{\text{argmin}}[\text{RSS}(d_i, \theta, \tau, L)] \tag{21}$$

With these new optimized parameters $\hat{\theta}_i$, we compute $\text{RSS}(D, \hat{\theta}_i, \tau, L)$ which represents the error generated over the full domain D using the parameter estimate $\hat{\theta}_i$ for a specific value of our hyper-parameters τ and L. We then generate:

$$R_i(\tau, L) = -\frac{N}{2}\ln(2\pi) + \ln(\text{RSS}(D, \hat{\theta}_i, \tau, L) - 1) \tag{22}$$

where N is the total number of observation points in D. Once these are computed for each replicate, our cross-validation score for a value of τ is the average of these quantities:

$$R_{\text{CrossVal}}(\tau, L) = \frac{1}{2}\sum_{i=1}^{2} R_i(\tau, L) \tag{23}$$

The value of the hyper-parameters τ and L that maximize Eq. (23) will be used in our simulations.

4 Results

4.1 Cross-Validation

Figure 3 displays the result for the cross-validation scores (Eq. 23) for integer values of τ, the density-dependent fecundity delay parameter, ranging from 6 days to 24

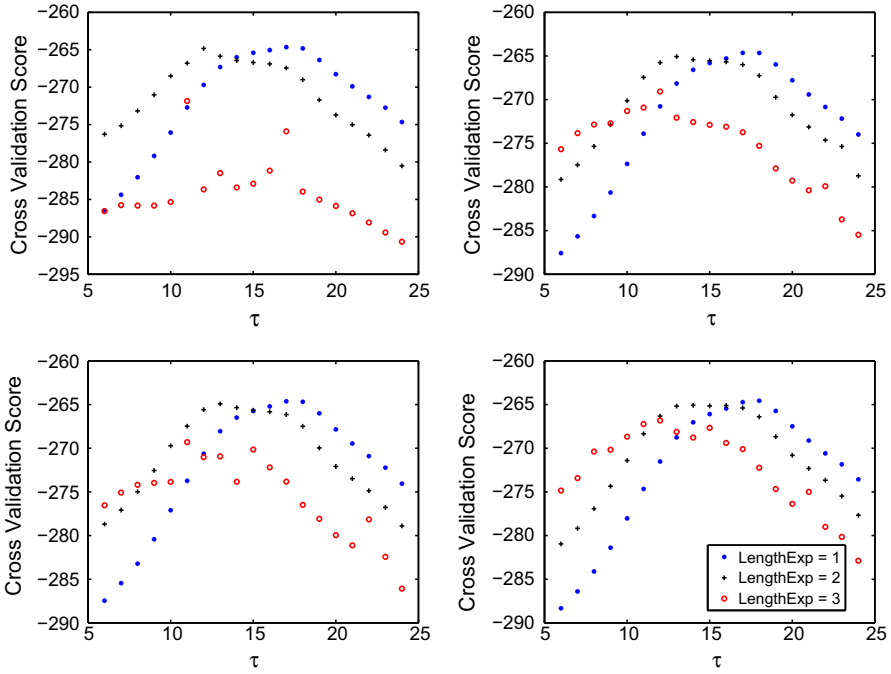

Fig. 3 (Color figure online) Cross-validation scores using the two replicates for various integer values of τ, the fecundity delay parameter and L, the exponent relating daphnid length to biomass. The upper left-hand corner represents the Adoteye et al. (2015b) food values of r, K and M_0, the lower left-hand corner represents the control food values of r, K and M_0, the upper right corner is for the medium food values of r, K and M_0, and the lower right corner contains the results for the low food values of$r$, K and M_0. For each food level, either $\tau = 17$ with $L = 1$ or $\tau = 12$ with $L = 2$ provides the best cross-validation score

days and L, the exponent relating daphnid length to biomass, ranging from 1 to 3. The four subfigures represent differing r and K values for the Adoteye et al. (2015b) length experiment (upper left), control food group (lower left), the medium food group (upper right) and the low food group (lower right). We found that L equal to 1 (with $\tau = 12 - 14$) or 2 (with $\tau = 17 - 18$) results in a maximal cross-validation score. This means that, in terms of generalizability, either combination of parameters is sufficient. We set $L = 2$ in order for biological feasibility, since daphnid length is related to biomass with an exponent value of 2–3 (de Roos et al. 1990). This then corresponds to a τ value of 12–14, depending on which r and K food values we are using.

4.2 Model Selection

In order to determine which food level to use, we examine the ability of each food level to fit the current data. We turn to the Akaike Information Criteria (AIC) score (Akaike 1974; Burnham and Anderson 2002), an unbiased measure of how well a model fits data. The AIC score, under a least-squares framework (Banks and Joyner 2017), is given by:

Table 3 Akaike weights for the two replicates over the four classes of food. Higher Akaike weights imply a better fit of the model to the data

Food group	Replicate 1	Replicate 2
Adoteye et al. (2015b) Food	0.5929	0.2618
Control food	0.1362	0.2543
Medium food	0.2558	0.2090
Low food	0.0151	0.2749

$$\text{AIC} = Nb \ln\left(\frac{\text{RSS}}{N} b\right) + Nb(1 + \ln(2\pi)) + 2(\kappa_\theta + 1) \tag{24}$$

where N represents the number of data observations, b represents the number of observables, in this case size class 1 and size class 2, κ_θ is the number of parameters being estimated, and RSS is the residual sum of squares. A lower AIC score implies higher accuracy (better model fit).

The AIC scores need to be corrected when there are few data points as compared to parameters being estimated. Since, for our data sets and parameters, $\frac{N}{\kappa_\theta} < 40$, we will instead use the AIC_C which is given by:

$$\text{AIC}_C = \text{AIC} + 2\frac{\tilde{p}(b + \kappa_\theta + 1)}{N - (b + \kappa_\theta + 1)} \tag{25}$$

where $\tilde{p}$ represents the total number of free parameters in the mathematical and statistical models. In our case, $\tilde{p} = \kappa_\theta + 2$, since we estimate σ_{0i}^2 in our statistical error model.

We are interested in determining whether there really is improvement in one model versus the other. To do this, we can calculate the probability of the correct model (Wagenmakers and Farrell 2004) using Akaike weights (Burnham and Anderson 2002).

In order to compute the Akaike weights, we need to determine the difference between the best AIC_C score:

$$\Delta_i(\text{AIC}_C) = \text{AIC}_{Ci} - \min \text{AIC}_C \tag{26}$$

The Akaike weights are computed using this measure of AIC_C differences as:

$$w_i(\text{AIC}_C) = \frac{\exp\left[-\frac{1}{2}\Delta_i(\text{AIC}_C)\right]}{\sum_{k=1}^{K} \exp\left[-\frac{1}{2}\Delta_k(\text{AIC}_C)\right]} \tag{27}$$

Note that $\sum_{k=1}^{K} w_k(AIC_C) = 1$, since the Akaike weights represent the probability that model i is the correct model. Therefore, the model with the higher Akaike weight is considered to be the better model (Wagenmakers and Farrell 2004).

Table 3 contains the resulting Akaike weights for the four food groups with $L = 2$ and the resulting τ value which minimized the cross-validation scores. It is apparent that there is no favored model for replicate 2, since the Akaike

weights are approximately the same. For replicate 1, there is not a strong favoritism for any specific food group; however, it appears that the Adoteye et al. (2015b) values of r, K, and M_0 generate a slightly better fit. For the remainder of simulations, unless otherwise stated, the hyper-parameters are $L = 2$, $\tau = 12$, and using r, K, and M_0 from the Adoteye et al. (2015b) food group. We note that a τ value of 12 has several biological interpretations, e.g., it is possible that changes in biomass take approximately four molt cycles to have an effect on fecundity. Alternatively, the delay may correspond to the approximate juvenile maturation time (McCauley et al. 2008). Further experimental work is needed to test these hypotheses.

Why do we not observe large differences in accuracy between models based on different food groups? Previous papers have argued that food quantity strongly influences growth, survival, and fecundity (de Roos et al. 1990; Ananthasubramaniam et al. 2011; Kooijman and Metz 1984). In contrast to the previous work (de Roos et al. 1990; Ananthasubramaniam et al. 2011; Kooijman and Metz 1984), the central focus of our efforts presented here is to determine a model that accurately fits population-level data from a density-dependent experimental scenario, where presumably higher population densities result in lower food quantity. Our findings seem to suggest that assuming a density-independent daphnid growth rate provides an approximation that results in accurate fits to population-level data. We note that the effect of density on survival and fecundity is modeled by Eqs. (4) and (5) and is estimated through parameters c_1 and q, respectively. Since $M(t)$ only appears in Eqs. (4) and (5), it is possible that estimating c_1 and q can compensate for differences in food group parameters, which only affect $M(t)$. Further experimental work should be done to measure food quantity, e.g,. algae content, in the microcosms in order to better estimate the relationship between daphnid biomass, growth, survival, and fecundity.

4.3 SPM Parameter Estimation and Uncertainty

Figure 4 displays the density-dependent SPM fit to the data for replicate 1 with optimized parameters. The fits are broken up into each size class as well as the total population. On the left side are the total population numbers at each day for each class and on the right is a surface representing dynamics of age, time, and population number. The data are shown with open circles and the model fit in a solid black line. The model solution for replicate one appears to fit each size class as well as the total population.

A similar plot for replicate 2 is shown in Fig. 5. We can see that in replicate 2, the optimized fit does not appear as accurate, especially with size class one during the early portion of the simulation. During this time, we can see that there is a sharp increase in size class one, which is even higher than the similar increase in replicate 1. Size class two, however, does appear to have an accurate fit.

The resulting parameters, their confidence intervals, and standard errors are in Table 4, separated into the first replicate (top) and second replicate (bottom). All parameters have nonnegative confidence intervals, which we require for biological

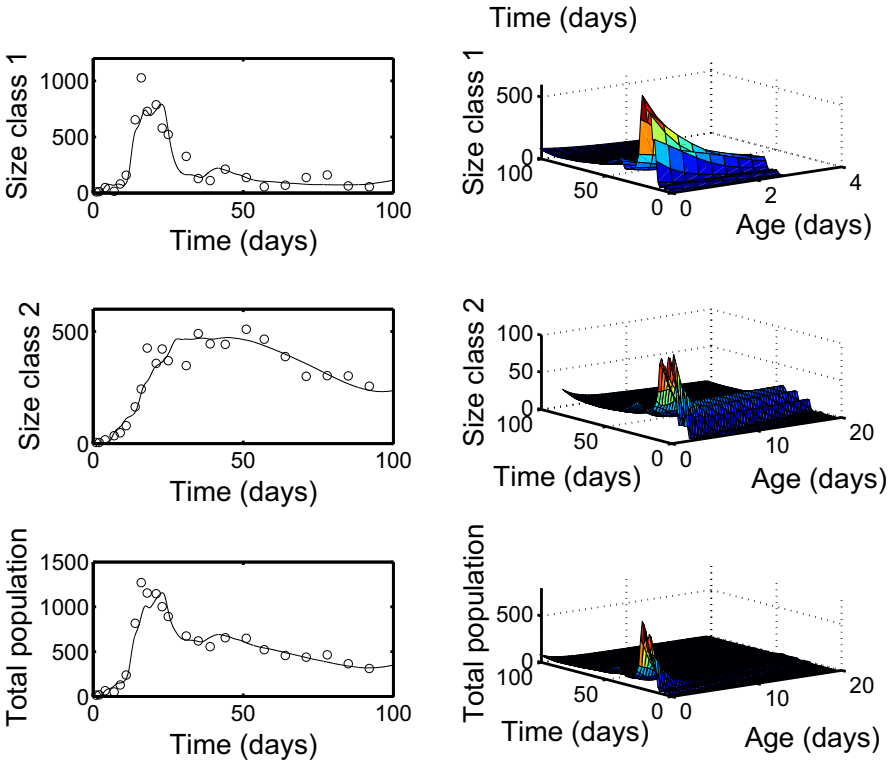

Fig. 4 (Color figure online) Density-dependent SPM fit to data for replicate 1. Daphnids separated into size class one (top), size class 2 (middle) and total population (bottom). On the left, the total number of daphnids in each size class per day, on the right a surface representing age, time and population number

relevance. The standard errors are relatively small. Although the optimized parameter q for replicate 2 is outside the range of the 95% confidence interval generated in replicate 1, the optimized parameter q for replicate 1 is inside the range of the 95% confidence interval generated in replicate 2. The parameter c_1 for each replicate remains outside of the others' confidence interval. Additional replicates would be useful in determining which set of parameters is more descriptive of population dynamics.

We would also like to examine the residuals for each replicate with respect to time and model value. This will help to insure that the statistical model chosen, of $\gamma = 0.5$ for size class 1 and $\gamma = 0$ for size class 2, is correct. Figure 6 displays the residuals for both replicate one (left) and replicate two (right). Within each subfigure, the left panels show residuals against time and the right panels show residuals against model value. The top figures represent size class one and the bottom figures represent size class two. The residuals for all cases appear to be evenly distributed, indicating that the choice of statistical error model is correct.

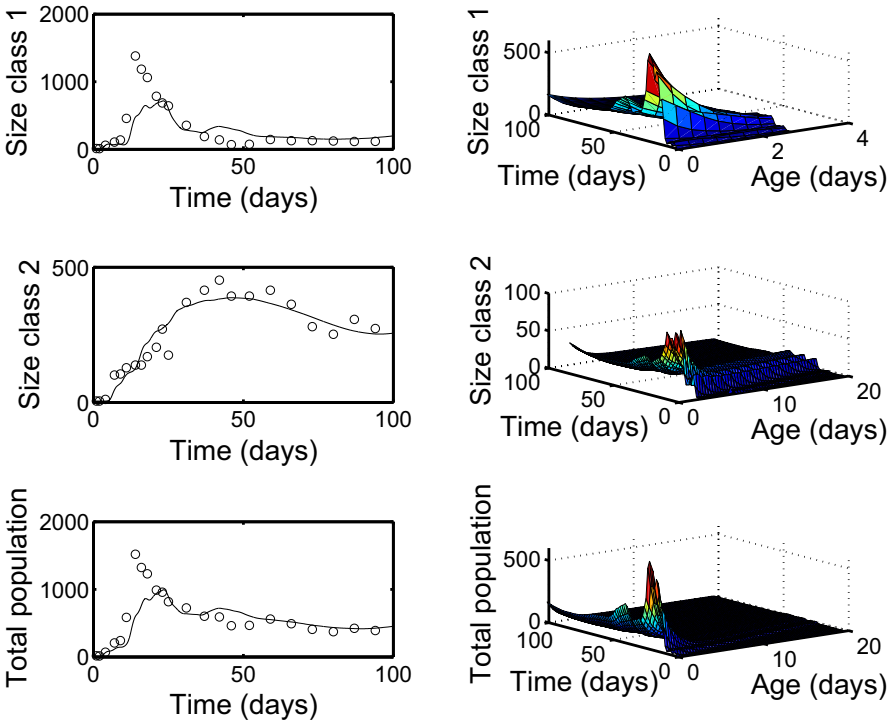

Fig. 5 (Color figure online) Density-dependent SPM fit to data for replicate 2. Daphnids separated into size class one (top), size class 2 (middle) and total population (bottom). On the left, the total number of daphnids in each size class per day, on the right a surface representing age, time and population number

Table 4 Optimal parameters, confidence intervals, and standard errors for replicates 1 and 2

Parameter	Estimate (Rep1)	95% CI (Rep1)	SE (Rep1)
q	156.8398	(106.7968, 206.8827)	25.6630
c_1	0.0185	(0.0168, 0.0202)	8.6934e−4
Parameter	Estimate (Rep2)	95% CI (Rep2)	SE (Rep2)
q	245.0448	(108.8946, 381.1950)	69.8206
c_1	0.0243	(0.0223, 0.0263)	0.0010

4.4 Sensitivity Analysis

We perform a local sensitivity analysis for the parameters for each replicate and each size class as well as the full population size. Figure 7 displays the results of this sensitivity analysis. Replicate one is shown in black, and replicate two is shown in red. The vertical dashed line is the time at which the daphnia population reaches its peak during the experiments and occurs at the same time for both replicates. Sensitivities were calculated using the complex-step method (Martins et al. 2000) and were corroborated with the finite differencing.

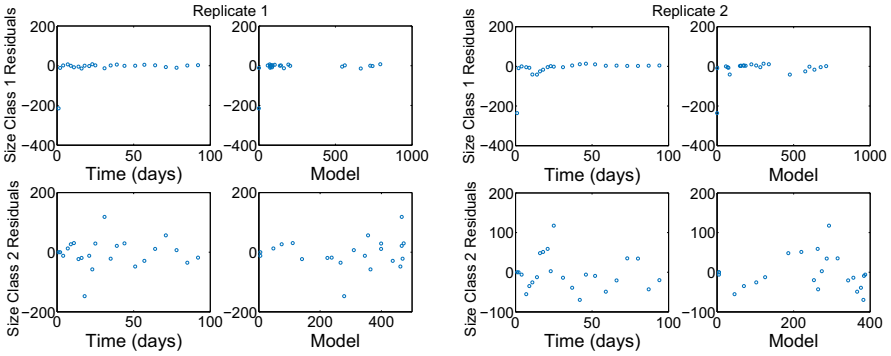

Fig. 6 (Color figure online) Residual plots for replicate one (left) and replicate two (right) for each class size and against time and model value. Residuals appear random, implying the statistical error model is sufficient

The left panels of Fig. 7 display the sensitivity of the solutions with respect to q, which is present in the density-dependent fecundity rate (Eq. 5). Increasing q leads to higher fecundity rates and, thus, higher population levels for all size classes. Since q is heavily involved in the fecundity rate, it is sensible that there are slight oscillations in the sensitivities, since the daphnia give birth every third day, meaning that those days may be more sensitive to changes in parameter q. We varied our adjoint step size to ensure that the sensitivities converged and the oscillations were not due to numerical instability.

The right panels in Fig. 7 portrays the sensitivity of the solutions with respect to c_1. The parameter c_1 is the linear relationship between density-dependent mortality and biomass, $M(t)$ (Eq. 4). For the total population size, we see that increasing c_1 results in lower population levels, which is sensible, as it increases the density-dependent death rate. However, the dynamics are very different depending on whether we are looking at size class 1 or size class 2. For size class 1, increasing c_1 results in lower size class 1 populations for approximately the first 30 days of the experiment, after which increasing c_1 results in higher size class 1 populations. This is also somewhat intuitive since populations of size class 1s are very large in the first 30 days, meaning that the biomass is quite large, which increases the death rate. However, in later times, population levels are low, which means that increasing c_1 may not be enough to overcome the small values of $M(t)$.

In general, the sensitivities for replicate 1 and replicate 2 have similar overall shapes, although replicate 2 tends to show more oscillatory behavior. We hypothesize the oscillations, mostly present in size class 1, are related to the movement of individuals from size class 1 to size class 2 (when they reach 3 days old) and to the delay in the fecundity term in Eq. (5).

5 Discussion and Conclusions

We proposed a continuously structured population model that included both density-dependent and density-independent growth, fecundity, and mortality for *Daphnia magna* populations. The model that we proposed was used to fit longitudinal experi-

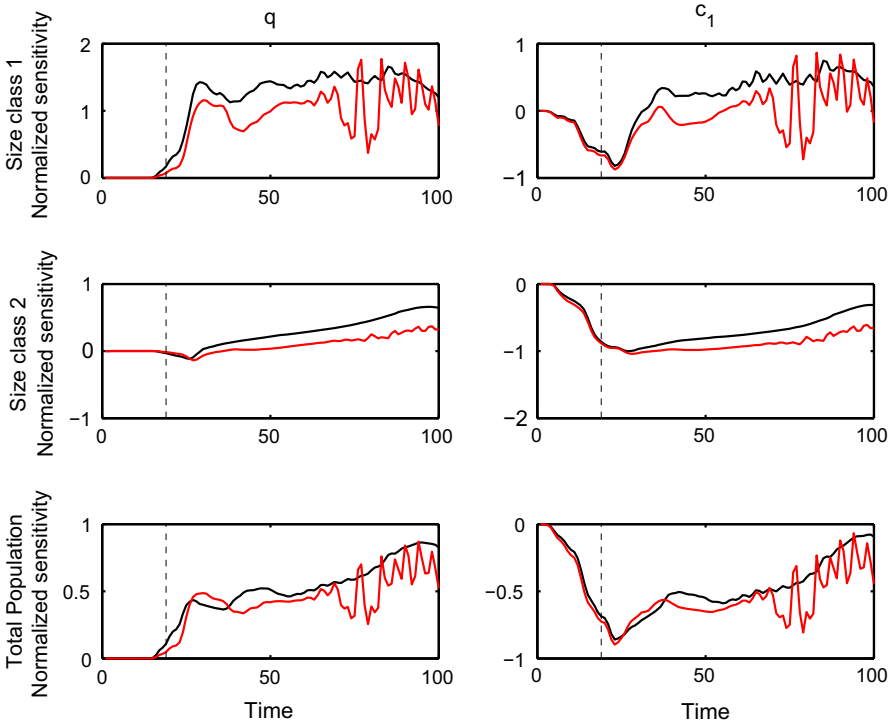

Fig. 7 (Color figure online) Sensitivity analysis for each parameter for each size class and total populations. Replicate one is shown in black, and replicate 2 is shown in red. The vertical dashed line represents the time at which the population reaches its maximum in the experiments

mental data of population dynamics of *D. magna*. We performed an individual study of 84 daphnids at three different food levels to determine the effect of food quantity on major axis length. We discovered that the growth rate of the various food restriction groups was not significantly different; however, the carrying capacity, i.e., adult daphnid size, was significantly different. The model was fit to data using a generalized least-squares framework. We also generated parameter estimates and their associated confidence intervals. For the two parameters that were estimated, we performed local sensitivity analysis to further understand the effect of changing their values.

In addition to our current model, we also proposed a slight variation in the density-dependent death term, changing the linear relationship between biomass and density-dependent death rate to a hill function. This results in changing Eq. (4) to

$$\mu_{\text{dep}}(a, M(t)) = 1 + \frac{c_1 M(t)^{h_1}}{c_2^{h_1} + M(t)^{h_1}} \frac{c_3^{h_2}}{c_3^{h_2} + a^{h_2}}. \tag{28}$$

where c_2 and h_1 are optimized along with q and c_1. This change allows further range of flexibility in how the density-dependent death rate depends on the total biomass, $M(t)$. We performed the same optimization as outlined above including calculating

Table 5 SE values for various data collection schedules for Replicate 1 and Replicate 2 for the optimized parameters

Collection schedule (# time points)	Replicate 1 SE q(156.8398)	Replicate 1 SE c_1(0.0185)	Replicate 2 SE q(245.0448)	Replicate 2 SE c_1(0.0243)
M–F weekly (67)	13.3679	5.1441e−04	39.8505	5.3772e−04
M/W/F weekly (40)	17.0327	6.5928e−04	50.7035	6.9229e−04
Tu/Th weekly (27)	21.5716	8.2271e−04	64.4546	8.5388e−04
M/F weekly (26)	21.0434	8.0096e−04	64.5870	8.4383−04
Weekly (14)	28.9971	0.0011	92.3124	0.00102
Our schedule (25)	25.6630	8.6934e−04	69.8206	0.0010

the cross-validation score, model selection, optimizing parameters, and determining confidence intervals. Our results indicate that this model may be over-parameterized since c_1, c_2, and h_1 had large standard errors and their confidence intervals included negative numbers. AIC scores indicated that the 4-parameter model did not fit the data better than the 2-parameter model. Full results of this analysis can be found in Rutter et al. (2016).

There are still several avenues that can be explored with this information. Although we did not notice much improvement by incorporating the various food levels, we note that, during longitudinal experiments, food is not at a constant level. Future experimental work will include measurements of algae concentration, so we can incorporate a dynamic carrying capacity dependent on food availability. These measurements will also allow us to model the algae concentrations.

Although we showed that our model could accurately fit population-level data, we would be interested in determining whether or not our model is sufficient for prediction. Future work includes evaluating the model's ability to predict future daphnid populations and comparing to current state-of-the-art daphnid population models.

Data collection for this experiment was labor intensive, and we hypothesized whether we could have obtained a similar quality fit with less frequent data collection. To this end, we simulated plausible data collection schedules including reducing the total number of data points to examine which points were most important to determining parameter estimates. Our results suggest that such frequent data collection is unnecessary but that consistent collection of data may be more important in reducing standard errors (SEs). We examined the standard errors for weekday data collections (M–F every week), 3x a week collection (M/W/F every week), 2x a week collection (M/F or T/T every week) and once weekly collection. SEs were calculated using methods described in Sect. 3.2. The SEs for all of these alternative schedules, with the exception of once weekly, were lower than the SE obtained with our collection schedule (M/W/F for first 3 weeks, thereafter weekly), even though, in some cases, the total number of data points collected was similar (Table 5).

Recent work has shown that perturbing biological systems away from equilibrium result in a large increase in data information content (Baraldi et al. 2014). By perturbing the system in an experimentally controlled manner, we may be able to decrease the

standard errors and uncertainties in parameter estimates (Adoteye et al. 2015c). Due to the large normalized standard errors present in our 4-parameter model, as well as the non-overlapping confidence intervals in our 2-parameter model, it may be possible to design optimal perturbations in our experimental procedure that would lower our standard errors. Future work will include an in-depth analysis of optimal design of our experiments for this purpose.

Acknowledgements This research was supported in part by the Air Force Office of Scientific Research under Grant Number AFOSR FA9550-15-1-0298, in part by the National Science Foundation under NSF Grant Number DMS-0946431, and in part by the EPA under US EPA STAR Grant RD-835165.

References

Adoteye K, Banks H, Flores KB, LeBlanc GA (2015a) Estimation of time-varying mortality rates using continuous models for *Daphnia magna*. Appl Math Lett 44:12–16

Adoteye K, Banks HT, Cross K, Eytcheson S, Flores KB, LeBlanc GA, Nguyen T, Ross C, Smith E, Stemkovski M et al (2015b) Statistical validation of structured population models for *Daphnia magna*. Math Biosci 266:73–84

Adoteye K, Banks HT, Flores KB (2015c) Optimal design of non-equilibrium experiments for genetic network interrogation. Appl Math Lett 40:84–89

Akaike H (1974) A new look at the statistical model identification. IEEE Trans Autom Control 19(6):716–723

Ananthasubramaniam B, Nisbet RM, Nelson WA, McCauley E, Gurney WS (2011) Stochastic growth reduces population fluctuations in Daphnia-algal systems. Ecology 92(2):362–372

Ankley GT, Bennett RS, Erickson RJ, Hoff DJ, Hornung MW, Johnson RD, Mount DR, Nichols JW, Russom CL, Schmieder PK et al (2010) Adverse outcome pathways: a conceptual framework to support ecotoxicology research and risk assessment. Environ Toxicol Chem 29(3):730–741

Baldwin WS, LeBlanc GA (1994) Identification of multiple steroid hydroxylases in *Daphnia magna* and their modulation by xenobiotics. Environ Toxicol Chem 13(7):1013–1021

Banks H, Davis JL (2007) A comparison of approximation methods for the estimation of probability distributions on parameters. Appl Numer Math 57(5):753–777

Banks HT, Joyner ML (2017) AIC under the framework of least squares estimation. Appl Math Lett 74:33–45

Banks HT, Tran H (2009) Mathematical and experimental modeling of physical and biological processes. CRC Press, Boca Raton

Banks H, Banks JE, Dick LK, Stark JD (2007) Estimation of dynamic rate parameters in insect populations undergoing sublethal exposure to pesticides. Bull Math Biol 69(7):2139–2180

Banks JE, Dick L, Banks H, Stark JD (2008) Time-varying vital rates in ecotoxicology: selective pesticides and aphid population dynamics. Ecol Model 210(1):155–160

Banks H, Davis JL, Ernstberger SL, Hu S, Artimovich E, Dhar AK (2009) Experimental design and estimation of growth rate distributions in size-structured shrimp populations. Inverse Probl 25(9):095003

Banks HT, Hu S, Thompson WC (2014) Modeling and inverse problems in the presence of uncertainty. CRC Press, Boca Raton

Banks HT, Catenacci J, Hu S (2015) Use of difference-based methods to explore statistical and mathematical model discrepancy in inverse problems. J Inverse Ill-posed Probl 24(4):413–433

Banks HT, Everett RA, Hu S, Murad N, Tran HT (2016) Mathematical and statistical model misspecifications in modelling immune response in renal transplant recipients. Inverse Probl Sci Eng 1–18

Baraldi R, Cross K, McChesney C, Poag L, Thorpe E, Flores KB, Banks H (2014) Uncertainty quantification for a model of HIV-1 patient response to antiretroviral therapy interruptions. Technical Report CRSC-TR13-13, Center for Research in Scientific Computation, N C State University, Raleigh, NC, Oct, 2013. In: 2014 American control conference, IEEE, pp 2753–2758

Burnham KP, Anderson DR (2002) Model selection and multimodel inference: a practical information-theoretic approach. Springer, New York

Caswell H (1989) Matrix population models: construction, analysis, and interpretation. Sinauer Associates, Sunderland
Caswell H (ed) (2005) Food webs: from connectivity to energetics. Advances in ecological research, vol 36. Elsevier Academic Press, San Diego
Council NR (2013) Assessing risks to endangered and threatened species from pesticides. The National Academies Press, Washington
Davidian M, Giltinan DM (1995) Nonlinear models for repeated measurement data, vol 62. CRC Press, Boca Raton
de Roos AM, Metz JAJ, Evers E, Leipolt A (1990) A size dependent predator-prey interaction: Who pursues whom? J Math Biol 28(6):609–643
Diekmann O, Gyllenberg M, Metz J (2007) Physiologically structured population models: towards a general mathematical theory. Springer, Berlin
Diekmann O, Gyllenberg M, Metz J, Nakaoka S, de Roos AM (2010) Daphnia revisited: local stability and bifurcation theory for physiologically structured population models explained by way of an example. J Math Biol 61(2):277–318
El-Doma M (2011) Stability analysis of a size-structured population dynamics model of Daphnia. Int J Pure Appl Math 70(2):189–209
El-Doma M (2012) A size-structured population dynamics model of Daphnia. Appl Math Lett 25(7):1041–1044
Ellner SP, Guckenheimer J (2011) Dynamic models in biology. Princeton University Press, Princeton
Ellner SP, Childs DZ, Rees M (2016) Data-driven modelling of structured populations: a practical guide to the integral projection model. Springer, Berlin
Erickson RA, Cox SB, Oates JL, Anderson TA, Salice CJ, Long KR (2014) A Daphnia population model that considers pesticide exposure and demographic stochasticity. Ecol Model 275:37–47
Farkas JZ, Hagen T (2007) Linear stability and positivity results for a generalized size-structured Daphnia model with inflow. Appl Anal 86(9):1087–1103
Finkel DE, Kelley CT (2004) Convergence analysis of the direct algorithm. Optim Online 14(2):1–10
Goser B, Ratte HT (1994) Experimental evidence of negative interference in *Daphnia magna*. Oecologia 98(3–4):354–361
Hanson N, Stark JD (2011) A comparison of simple and complex population models to reduce uncertainty in ecological risk assessments of chemicals: example with three species of Daphnia. Ecotoxicology 20(6):1268–1276
Keyfitz N, Caswell H (2005) Applied mathematical demography, 3rd edn. Springer, New York
Kooijman SALM, Metz JAJ (1984) On the dynamics of chemically stressed populations: the deduction of population consequences from effects on individuals. Ecotoxicol Environ Saf 8(3):254–274
Kramer VJ, Etterson MA, Hecker M, Murphy CA, Roesijadi G, Spade DJ, Spromberg JA, Wang M, Ankley GT (2011) Adverse outcome pathways and ecological risk assessment: bridging to population-level effects. Environ Toxicol Chem 30(1):64–76
LeBlanc GA, Wang YH, Holmes CN, Kwon G, Medlock EK (2013) A transgenerational endocrine signaling pathway in crustacea. PLoS ONE 8(4):e61715
Leslie PH (1945) On the use of matrices in certain population mathematics. Biometrika 33(3):183–212
Martins JRRA, Kroo IM, Alonso JJ (2000) An automated method for sensitivity analysis using complex variables. In: Proceedings of the 38th AIAA aerospace sciences meeting
McCauley E, Nelson WA, Nisbet RM (2008) Small-amplitude cycles emerge from stage-structured interactions in Daphnia-algal systems. Nature 455(7217):1240–1243
Nelson WA, McCauley E, Nisbet RM (2007) Stage-structured cycles generate strong fitness-equalizing mechanisms. Evol Ecol 21(4):499–515
Nisbet RM, Gurney WSC (1983) The systematic formulation of population models for insects with dynamically varying instar duration. Theor Popul Biol 23(1):114–135
Olmstead AW, LeBlanc GA (2007) The environmental-endocrine basis of gynandromorphism (intersex) in a crustacean. Int J Biol Sci 3(2):77–84
Preuss TG et al (2009) Development and validation of an individual based *Daphnia magna* population model: the influence of crowding on population dynamics. Ecol Model 220(2):310–329
Rider CV, LeBlanc GA (2005) An integrated addition and interaction model for assessing toxicity of chemical mixtures. Toxicol Sci 87(2):520–528

Rutter EM, Banks HT, LeBlanc G, Flores KB (2016) Continuous structured population models for *Daphnia magna*. Technical Report CRSC-TR16-16, Center for Research in Scientific Computation, N C State University, Raleigh, NC, Dec

Shampine L (2005) Solving hyperbolic pdes in matlab. Appl Numer Anal Comput Math 2(3):346–358

Sinko JW, Streifer W (1967) A new model for age-size structure of a population. Ecology 48(6):910–918

Wagenmakers E, Farrell S (2004) AIC model selection using Akaike weights. Psychon Bull Rev 11(1):192–196

Wang HY, Olmstead AW, Li H, LeBlanc GA (2005) The screening of chemicals for juvenoid-related endocrine activity using the water flea *Daphnia magna*. Aquat Toxicol 74(3):193–204

Wang YH, Kwon G, Li H, LeBlanc GA (2011) Tributyltin synergizes with 20-hydroxyecdysone to produce endocrine toxicity. Toxicol Sci 123(1):71–79

Wood S (1994) Obtaining birth and mortality patterns from structured population trajectories. Ecol Monogr 64(1):23–44